Int J Adv Manuf Technol (2017) 90:1835–1844
DOI 10.1007/s00170-016-9484-5

ORIGINAL ARTICLE

An experimental study on the creep feed grinding of narrow deep grooves of stainless steel

Yanyan Bai[1,2] · **Ming Lv**[1,2] · **Wenbin Li**[1,2] · **Guoxing Liang**[1,2]

Received: 8 April 2016 / Accepted: 15 September 2016 / Published online: 2 October 2016

Abstract Experiments were carried out machining SUS321 stainless steel workpieces using a single-layer electroplated cubic boron nitride (CBN) wheel; a WinTec MV-45 machining center and creep feed grinding following orthogonal test method were used. Narrow deep grooves were machined. The surface roughness R_a values of the groove side walls were collected and analyzed. The influence of grinding parameters (including wheel speed, feed rate, and cutting depth) on the surface roughness of the grooves was studied. The result showed that the feed rate has the most significant influence on the surface roughness R_a values of the narrow deep groove, the influence of the wheel speed on the surface roughness R_a values is the second, and the effect of the cutting depth on the surface roughness R_a values is the least. The optimum parameters were achieved by orthogonal experiment optimum design and taking v_w = 1.5 mm/min, a_p = 5 mm, n = 7000 rpm for grinding SUS321 stainless steel. A model predicting the surface roughness R_a values of the machined grooves was established by processing the collected data by partial least square regression. The predictions made by the model match well with the experimental data, and thus, the model can be used to predict the surface quality/roughness in future grinding.

✉ Ming Lv
lvmingtyut@126.com

[1] College of Mechanical Engineering, Taiyuan University of Technology, Taiyuan 030024, China

[2] Shanxi Key Laboratory of Precision Machining, Taiyuan 030024, China

Keywords Creep feed grinding · Narrow deep groove · Stainless steel · Orthogonal test · Surface roughness · Partial least square regression

1 Introduction

Stainless steel is a typical hard processing material, and abrasive dusts adhere to the blade seriously during its grinding process. So it is easy to cause the grinding wheel to block, which has a great effect on the quality of machined surface and decreases cutting efficiency. In recent years, the development of high-speed grinding technology provides a new way for the grinding of stainless steel. Considerable progress has been made in the study on the grinding process of stainless steel. Wang et al. [1] conducted the stainless steel wire tip grinding experiments in a Chevalier Model Smart-B818 three-axis computer numerical control (CNC) surface grinding machine to study the grinding forces, wire tip deflection, and surface roughness. Ohmori et al. [2] investigated in detail a stainless steel mirror-finished surface obtained by a high-precision grinding process using some advanced surface analyzing techniques, and found that ground surfaces exhibited superior surface properties including hardness, tribilogical and fatigue properties, corrosion, and high-temperature oxidation resistance. Manimarana et al. [3] conducted grinding experiments on stainless steel 316L to study the grinding force and surface roughness. Zhou et al. [4] ground duplex stainless steel (DSS) 2304 to study the effect of abrasive grit size, grinding force, and lubrication on the surface integrity. Baptista et al. [5] studied the fatigue behavior in welded joints of stainless steels (Austenitic 304L and Duplex S31803 type) treated by weld toe grinding. Hadad and Hadi [6] did the surface grinding tests for hardened stainless steel under dry, MQL, and fluid grinding conditions. The results showed that

Table 1 Chemical compositions of SUS321 stainless steel

Element	C	Si	Mn	P	S	Cr	Ti	Ni
Chemical composition/wt%	0.08	1	2	≤0.045	≤0.030	17.00–19.00	5C-0.70	9.00–12.00

for MQL grinding of hardened stainless steel, not only a superior surface finish and quality are obtained but also the tangential grinding forces are lower.

In any grinding process, the surface roughness of the machined piece, which is affected by grinding conditions like depth of cut, feed rate, wheel speed, the lubrication effectiveness, and workpiece characteristics such as hardness, toughness and machinability, etc. is one of the most important factors in assessing the quality of the process. Surface roughness influences several functional attributes of parts, such as contact area and characteristics causing surface friction, wearing, light reflection, heat transmission, ability of distributing and holding a lubricant, load bearing capacity, and fatigue resistance [7]. Therefore, the desired surface roughness is usually specified and the appropriate processes are selected to reach the required quality levels.

In the past several years, many researches have been done about investigating the influence of grinding parameters on surface roughness in order to achieve better surface finishes, and many empirical models predicting the surface roughness of ground components under some grinding conditions have been established. Gopal and Rao [8] conducted experiments of grinding of silicon carbide (SiC) to study the effects of wheel parameters (mesh size and grain density) and grinding parameters (depth of cut and feed) on the surface roughness and surface damage. The results indicated that the parameters feed rate, depth of cut, and grit size are the primary influencing factors which affect the surface integrity of SiC during grinding. The surface roughness model was developed using the experimental data considering only the significant parameters. Optimal grinding conditions were also obtained for maximization of material removal using surface roughness and percentage damage as constraints. Rudrapati et al. [7] made experiments by Box-Behnken design matrix and investigated the influence of machining parameters as infeed, longitudinal feed, and work speed on surface roughness in traverse cut cylindrical grinding of stainless steel material (grade SS410). The results showed that surface roughness R_a values generally decrease with an increase in longitudinal feed and increase with an increase in infeed and work speed. Infeed, squared combinations of both longitudinal feed and work speed, and interaction effect infeed-longitudinal feed and longitudinal feed-work speed are found to be the most significant for surface roughness. Mathematical modeling had also been done by response surface methodology (RSM) to develop the relationship between process parameters and surface roughness R_a values. Lin et al. [9] investigated the effects of grinding parameters and grinding wheels on the grinding performance of in situ TiB2/Al composites employing down-grinding style with emulsified lubrication. The results showed that increasing workpiece speed and grinding depth result in the increase of surface roughness, and the most significant grinding parameters on the grinding quality of in situ TiB2/Al composites are wheel speed and grinding depth, while the effect of workpiece speed on the surface roughness is inconspicuous. Yao et al. [10] conducted the experiments of grinding surface integrity using a SA and a CBN wheel, respectively, and compared and analyzed the surface roughness and topography of ground surface with different grinding parameters. The results showed that the SA wheel is suitable for grinding Inconel718, and the grinding depth has a great effect on the surface integrity in grinding Inconel718. It can also be concluded that better surface can be achieved by using a SA wheel, and taking such grinding parameter as a_p = 0.005 mm, v_w = 16 m/min, and v_s = 25 m/s for grinding Inconel718. Fredj et al. [11] conducted the grinding tests in down cut plunge surface grinding mode. For all tests, a 48 runs design of experiment (DoE) rotatable central composite design was selected concerning the grinding parameters, table speed, depth of cut, grinding wheel, grain mesh size, dressing depth, and the number of passes. The results showed that only the table speed, the depth of cut, the dressing depth, the interaction depth of cut, and the number of passes are significant in the case of R_a. An approach combining the application of the DoE and the neural network methods was developed to establish accurate models for ground surface roughness prediction.

Table 2 Mechanical properties of SUS321 stainless steel

Property	Tensile strength, σ_b (MPa)	Yield strength, $\sigma_{0.2}$ (MPa)	Elongation, δ_5 (%)	Reduction of area, ψ (%)	Hardness, HBR
Value	≥520	≥205	≥40	≥50	≤83

Narrow deep groove is a special type of groove structure with the width of groove to be less than 4 mm and the ratio of the depth over the width (of groove) to be greater than 2. Such grooves are often used on some key parts in the aviation and automotive field. For example, the rotor slot of the rotor pump is a typical part with narrow deep grooves. According to the technical requirements of the manufacturer, the surface roughness R_a value of the slot wall is 0.4 μm. Machining such narrow deep grooves of high precision has been proven to be challenging. In recent years, the creep feed grinding technology has shown a unique advantage in the process of machining narrow deep grooves [12–16]. Referring back to the rotor pump, when transporting corrosive material, rotor material must be a corrosion-resistant material, such as SUS321 austenitic stainless steel, which has good low-temperature strength as well as good elevated temperature strength and is widely used in various fields of chemical industry and light industry.

Although there exist many literatures relating the grinding parameters with the part roughness and some models for the surface roughness generated by the grinding process, they are not the results of the creep feed grinding of SUS321 stainless steel. In order to find the influence of the grinding parameters such as cutting depth, feed rate, and wheel speed on the surface roughness and achieve precise prediction of surface roughness for effective control of grinding quality during the creep feed grinding of SUS321 stainless steel, experiments were conducted by an orthogonal test method in this work. A cubic boron nitride (CBN) grinding wheel with a single-layer electroplating was used to perform the creep feed grinding of a SUS321 stainless steel workpiece. Straight grooves with a width of 2 mm and a depth of 8, 12, and 5 mm were machined. Each groove was machined according to different grinding parameters. The relationship between the surface roughness R_a values of the walls of the grooves and the grinding parameters is investigated. The effect of grinding parameters on the surface roughness/quality is studied to make a prediction model of the surface roughness of the machined narrow deep grooves.

2 Experimental

2.1 Experimental conditions

A cylindrical sample of SUS321 austenitic stainless steel with a size of 100 mm (length) by 20 mm (diameter) was selected for this investigation. The chemical composition and mechanical properties of SUS321 austenitic stainless steel are given in Table 1 and Table 2, respectively. The narrow deep groove grinding experiments were carried out in a WinTec MV-40 machining center with a maximum operational spindle speed of 10,000 rpm using the setup shown in Fig. 1. The single-layer electroplated CBN wheel with 45 steel as the hub body was mounted on the spindle of the machining center by a special toolholder. The wheel size is about 180 mm in diameter and 1.8 mm in depth. The width of the coating is 5 mm. The average grit size is 120 mesh. The volume fraction of CBN in the coating is 22.3 %. The workpiece is secured by a bench vise mounted on the machine table. Processing sketch map (down) is shown in Fig. 2. The grinding experiments were performed in dry condition. After the grinding process of the narrow deep grooves on the SUS321 stainless steel bar, each groove bottom was cut by a wire electrical discharge machining (WEDM) to observe surface morphology of the groove side walls by scanning electron microscope (SEM). The surface roughness R_a values of the side walls of the narrow deep grooves were measured using a TR220 contact type surface profilometer.

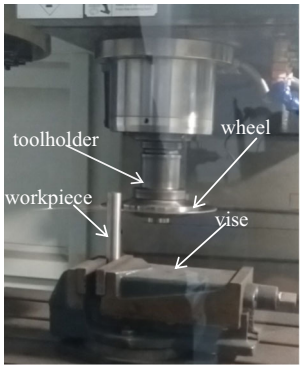

Fig. 1 Experiment setup for grinding the narrow deep grooves

2.2 Experimental program

The surface roughness in a creep feed grinding process is affected by many factors such as the rigidity of the machine tool, the material of the workpiece, the grit material, the grit size, the cooling condition, and the grinding parameters. In order to investigate the influence of the grinding parameters (including peripheral wheel speed, feed rate, and cutting depth) on the ground surfaces of the narrow deep grooves, the grinding experiments were conducted in this paper by an orthogonal test method. The orthogonal test is an effective measurement to assay the comprehensive effect of multiple

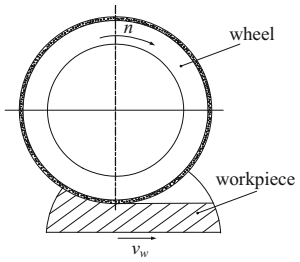

Fig. 2 Processing sketch map (down)

Table 3 The factors and levels of the orthogonal experiment

Level	Factor		
	Feed rate v_w (A) (mm/min)	Cutting depth a_p (B) (mm)	Wheel speed n (C) (rpm)
1	1	5	3000
2	1.2	8	4500
3	1.5	12	7000

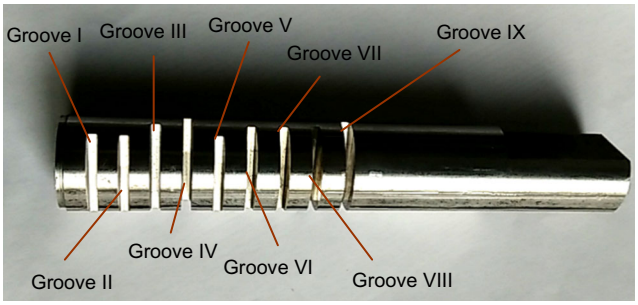

Fig. 3 Machined workpiece

factors [17]. Table 3 lists the factors and levels of the orthogonal experiment in which three grinding parameters including (A) feed rate, (B) cutting depth, and (C) wheel speed were selected. Each parameter has three levels to be optimized. For the interaction between the factors is ignored, and three factors are selected, $L_9(3^4)$ is the suitable orthogonal array for the experiment [18–20], as is shown in Table 4. Nine trials were carried out according to the $L_9(3^4)$ array to machine nine narrow deep grooves to complete the optimization process. Each row of orthogonal array represents a run, which is a specific set of factor levels to be tested. The run order of the trials was randomized to avoid any personal or subjective bias. The machined workpiece was shown in Fig. 3. Each groove bottom was cut along its middle line by a wire electrical discharge machining (WEDM) to observe surface morphologies of the groove side walls by SEM. The surface roughness R_a values of the side walls of each groove were measured across the tool feed direction using a TR220 contact type surface profilometer. The sampling length was given by L = 0.25 mm, and the assessment length is given as 5L. The measurements were taken at different locations on each sample. The surface roughness R_a values written in the corresponding column of the orthogonal array were the average of the five measurements.

3 Results and discussion

From the experiment result in Table 4, it can be seen that the surface roughness R_a value of No. 9 trial is minimum for the left groove wall and the relatively optimal combination is $A_3B_3C_2$. It is also evident that the surface roughness R_a value of No. 5 trial is minimum for the right groove wall and the relatively optimal combination was $A_3B_1C_3$. But these tests may not be the optimum combination scheme. The deep analysis should be done to find the better scheme.

3.1 Range analysis

Range is the difference between the maximum and the minimum of the average of the target, and it is represented as R which can be obtained by:

$$R_i = \max\left(p_{i1}, \cdots p_{ij}, \cdots, p_{in}\right) - \min\left(p_{i1}, \cdots p_{ij}, \cdots, p_{in}\right) \quad (1)$$

where , p_{ij}(j = 1,2,…,n;i = 1,2,…,n) is the arithmetic mean of the test results obtained when the same levels j of the factor column i are selected in the orthogonal table. The value of R_i is used for evaluating the importance of the factors, i.e., a larger

Table 4 $L_9(3^4)$ orthogonal test array for the grinding experiments

Trial No.	Factor			Surface roughness R_a value (μm)	
	Feed rate v_w (A) (mm/min)	Cutting depth a_p (B) (mm)	Wheel speed n (C) (rpm)	left groove walls	right groove walls
1	1	5	3000	0.636	0.479
2	1.2	5	4500	0.891	0.604
3	1.5	8	3000	0.658	0.514
4	1	12	7000	0.842	0.583
5	1.5	5	7000	0.714	0.221
6	1.2	8	7000	1.109	0.509
7	1	8	4500	0.549	0.51
8	1.2	12	3000	1.038	0.502
9	1.5	12	4500	0.469	0.48

R_i means a greater importance of the factor. By comparing the different p_{ij} under the same factor, we can know that the trend of the influence of this factor on test result and get the optimum level of this factor column. The optimal combination of the whole experiment can be obtained by combining the optimal level of each factor column. The range analysis of the surface roughness R_a values of the left groove walls was shown in Table 5. The trend curve for each factor was shown in Fig. 4.

From the range analysis in Table 5 and the trend curve in Fig. 4, it can be seen that the feed rate has the greatest influence on the surface roughness R_a values of the left groove walls; the wheel speed has less influence on that, and the cutting depth has the smallest influence. The optimum combination is selected as $A_3B_1C_2$. The optimum parameters by orthogonal experiment optimum design are v_w = 1.5 m m/min, a_p = 5 mm, and n = 4500 rpm.

According to the surface roughness R_a values of the right groove walls in Table 4, the range analysis of the surface roughness R_a values of the right groove walls was obtained according to the formula (1) and shown in Table 6. The trend curve for each factor was shown in Fig. 5.

From Table 6 and Fig. 5, it can be found that the influence of grinding parameters on the surface roughness R_a values of the right groove walls is about the same as that on the surface roughness R_a values of the left groove walls: the effect of feed rate is the most significant, the second important factor is the wheel speed, and the effect of the cutting depth is the least. The optimum combination is selected as $A_3B_1C_3$, which is consistent with the result obtained through the intuitive analysis of the surface roughness R_a values of the right groove walls. So the verification test need not be carried out. The optimum parameters by orthogonal experiment optimum design are v_w = 1.5 mm/min, a_p = 5 mm, and n = 7000 rpm.

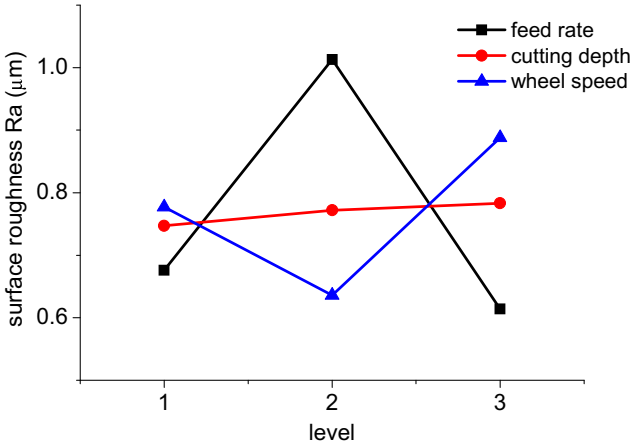

Fig. 4 Trend curve of the level on each factor of the left groove walls

3.2 Micrograph analysis of surface topography

The surface morphology of the grinding is mainly formed by the superposition of the groove marks generated by the interference of the abrasive cutting edge and the workpiece [21]. The typical SEM picture of the ground groove walls were shown in Fig. 6.

Table 5 Range analysis of the surface roughness R_a values of the left groove walls

Trial No.	Factor			Surface roughness R_a value of the left groove wall (μm)
	Feed rate v_w (A) (mm/min)	Cutting depth a_p (B) (mm)	Wheel speed n (C) (r/min)	
1	1	1	1	0.636
2	2	1	2	0.891
3	3	2	1	0.658
4	1	3	3	0.842
5	3	1	3	0.714
6	2	2	3	1.109
7	1	2	2	0.549
8	2	3	1	1.038
9	3	3	2	0.469
p_{11}, p_{21}, p_{31}	0.676	0.747	0.777	
p_{12}, p_{22}, p_{32}	1.013	0.772	0.636	
p_{13}, p_{23}, p_{33}	0.614	0.783	0.888	
Range R_1, R_2, R_3	0.399	0.036	0.252	
Order of the factor	A > C > B			
Optimum combination	$A_3B_1C_2$			

Table 6 Range analysis of the surface roughness R_a values of the right groove walls

Trial No.	Factor			Surface roughness R_a value of the right groove wall (μm)
	Feed rate v_w (A) (mm/min)	Cutting depth a_p (B) (mm)	Wheel speed n (C) (rpm)	
1	1	1	1	0.479
2	2	1	2	0.604
3	3	2	1	0.514
4	1	3	3	0.583
5	3	1	3	0.221
6	2	2	3	0.509
7	1	2	2	0.510
8	2	3	1	0.502
9	3	3	2	0.480
p_{11}, p_{21}, p_{31}	0.524	0.435	0.498	
p_{12}, p_{22}, p_{32}	0.538	0.511	0.531	
p_{13}, p_{23}, p_{33}	0.405	0.521	0.437	
Range R_1, R_2, R_3	0.133	0.086	0.094	
Order of the factor	A > C > B			
Optimum combination	$A_3B_1C_3$			

It can be seen from Fig. 6 (a)-(h) that the surface topographies of the narrow deep grooves machined with different grinding parameters are different. Obvious wide scratch, ditch, and lateral uplifts caused by grinding plow can be seen in the SEM pictures. Some of the apparent burns can be also seen on some of the pictures, and abrasive dusts adhere to the ground surface seriously, as shown in Fig. 6 (e), which indicates that with the increase of grinding wheel speed, the temperature of the grinding zone increases, and the ground surface gets burned. Grinding process is inevitably accompanied with the wear of grinding wheel. The CBN grinding debris shedding can be seen clearly in Fig. 6 (g).

It is also learned from Fig. 6 that the surface quality of the left and right groove walls were slightly different, which was consistent with the change rule of the surface roughness R_a values in Table 4. Taken together, the surface quality of Groove V is the best. The optimum combination is that v_w is given by 1.5 mm/min, a_p is given by 0.5 mm, and n is given by 7000 rpm. In this grinding condition, the peripheral wheel speed reached at 65.94 m/s, which belongs to high-speed grinding range.

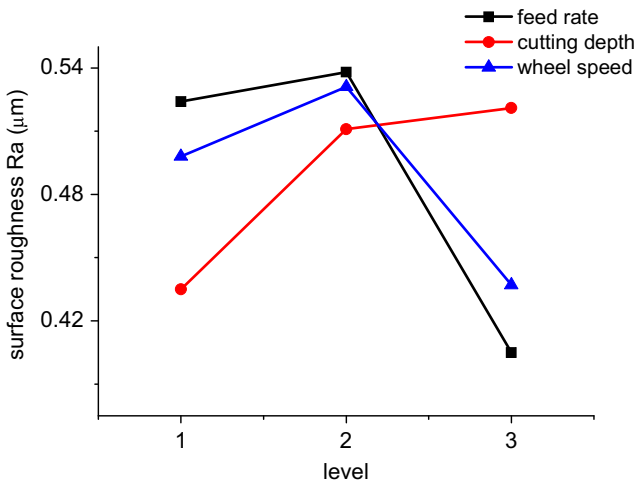

Fig. 5 Trend curve of the level on each factor of the right groove walls

4 Establishment of empirical prediction model of surface roughness

Similar to other machining processes, the surface roughness of grinding can be predicted theoretically by establishing the model of the interference between the grinding wheel and the workpiece.

Fig. 7 shows the ideal longitudinal profile of the surface formed by the abrasive cutting edge with different convex height, where the relevant parameters are labeled, and R_t represents the peak-valley roughness (also known as the overall roughness) [21]. If cutting depth $a_p > R_t$, then the cutting depth had no effect on the roughness. The arithmetic mean roughness R_a value is the mean deviation from the average roughness on the sampling length and is much smaller than R_t. Creep feed grinding in particular involves large depths of cut, ranging from 1 to 25 mm [21, 22]. In the process of narrow deep grooves of SUS321 stainless steel, this grinding technology was adopted. So the cutting depth a_p can be neglected when establishing the regression model of the surface roughness R_a value.

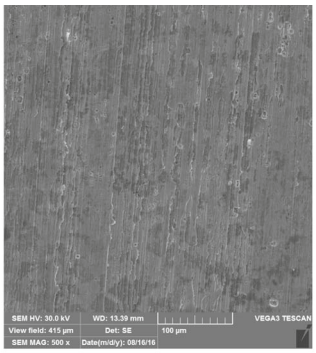

(a) the left groove wall of Groove I

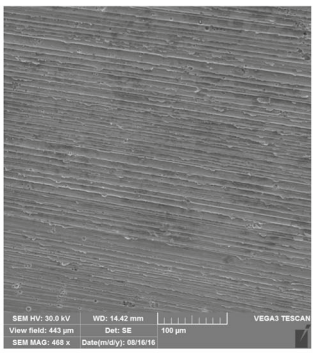

(b) the right groove wall of Groove I

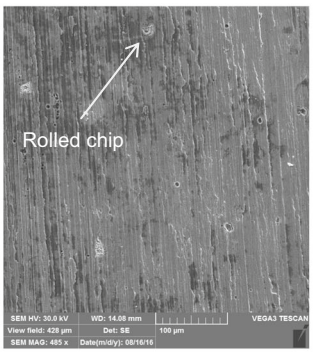

(c) the left groove wall of Groove V

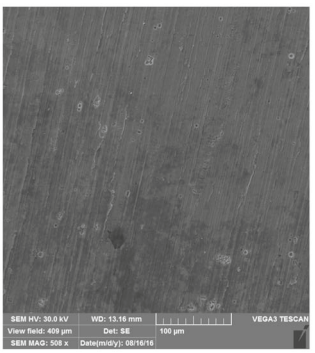

(d) the right groove wall of Groove V

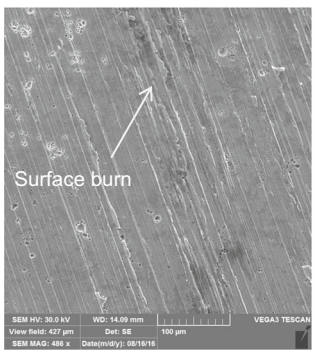

(e) the left groove wall of Groove VI

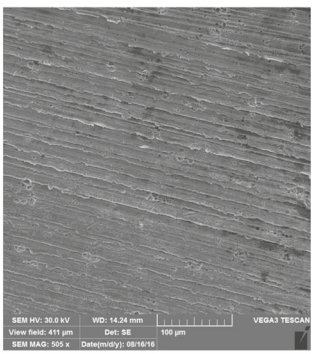

(f) the right groove wall of Groove VI

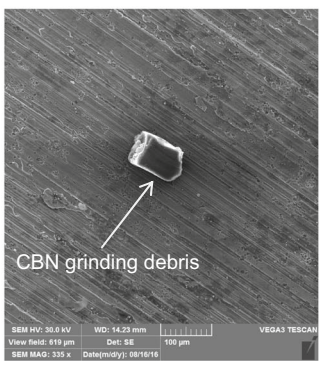

(g) the left groove wall of Groove IX

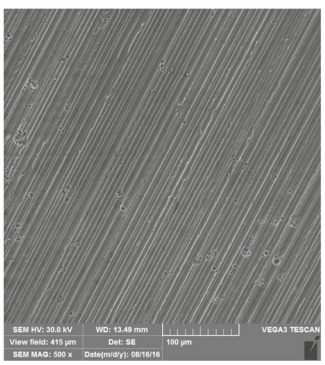

(h) the right groove wall of Groove IX

Fig. 6 Surface topography of the narrow-deep-groove walls of SUS321 stainless steel

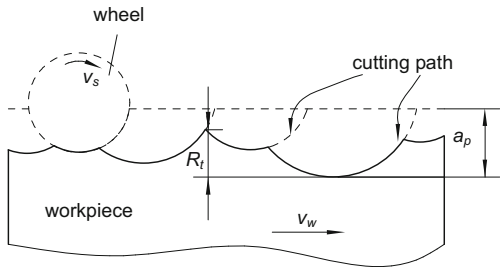

Fig. 7 Longitudinal theoretical profile formed by non-uniform grinding wheel topography

Table 7 Results of the regression statistics

Item	Result
Multiple *R*	0.97357
R square	0.94656
Adjusted *R* square	0.86089
Standard error	0.04079
Number of points	9

4.1 Establishment of the regression model

Partial least squares is a method for constructing predictive models, and it has been accepted and successfully applied in the control of industrial processes [23]. In this study, this technique was proposed to establish the regression model of surface roughness R_a value. There are two abnormal large values in the surface roughness R_a values of the left groove walls due to workpiece burn, so the regression analysis was carried out with the surface roughness R_a values of the right groove walls as the object of investigation.

A typical regression equation is as shown:

$$\widehat{y} = \beta_0 + \beta_1 x_1 + \beta_2 x_2 + \cdots + \beta_p x_p \quad (2)$$

where $\widehat{y}$ is the fitted value and β_0, β_1, . . ., and β_p are the estimations of the regression parameters.

The real value for y is

$$y = \beta_0 + \beta_1 x_1 + \beta_2 x_2 + \cdots + \beta_p x_p + \varepsilon \quad (3)$$

where y is the response parameter, x_1, x_2,…, x_p are the experimental factors, and$\varepsilon$is the random error.

According to the regression model in the above, relationship between the surface roughness R_a value and the grinding parameters can be expressed by a quadratic polynomial model as is shown:

$$R_a = -2.2874 + 3.3509 v_w + 0.00039 v_s - 1.0322 v_w^2 - 1.4867E\text{-}08 v_s^2 - 0.00021 v_w v_s \quad (4)$$

where v_w ,v_s is the feed rate (mm/min) and v_s is wheel speed (rpm), equivalent to the wheel speed n in Section 2 and 3.

From the above equation (4), it is easy to see that the feed rate (v_w) strongly affects surface roughness R_a value, followed by the wheel speed (v_s), whereas the interaction of feed rate and wheel speed has a little influence on surface roughness R_a value. This result is consistent with that obtained by the range analysis above.

Fig. 8 shows the trend of the surface roughness with the feed rate and the wheel speed. This trend is consistent with the experimental data. It is also known from Fig. 8 that the interaction between the feed rate and the wheel speed has a little effect on the surface roughness R_a value.

4.2 Test of regression model

After the quadratic polynomial model of surface roughness R_a value is established, it is necessary to test the regression effect by mathematical statistics methods such as R-test and F-test.

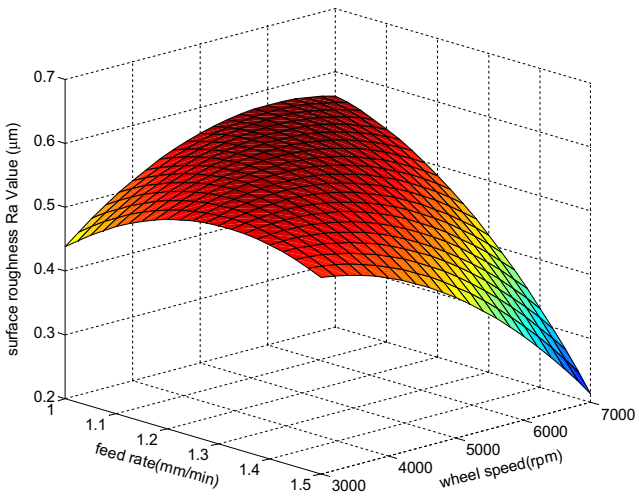

Fig. 8 Trend of the surface roughness with the feed rate and the wheel speed

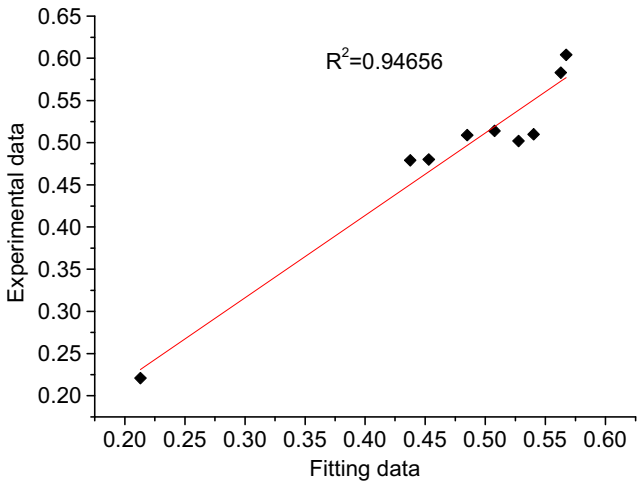

Fig. 9 Correlation between experimental data and the fitting data

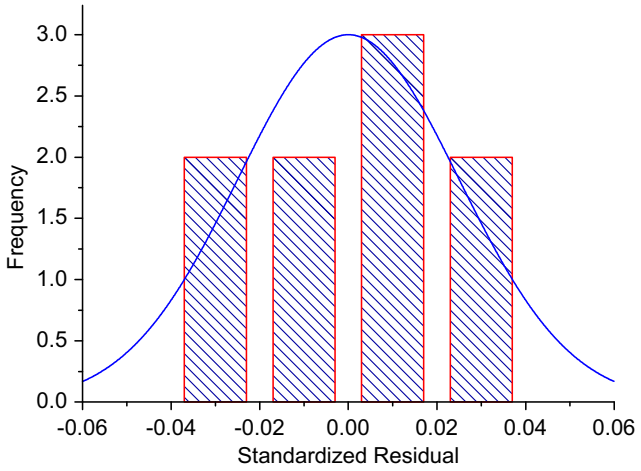

Fig. 10 Histogram of the residuals for the model

R-test is the goodness of fit test. The results of the regression statistics is shown in Table 7.

The coefficient of determination (R^2) is used to test the goodness of fit of the regression equation and the sample value. It is defined as follows:

$$R^2 = 1 - \frac{\sum \left(y_i - \widehat{y}_i\right)^2}{\sum \left(y_i - \overline{y}\right)^2} \tag{5}$$

where y_i is the predicted quality variable, y_i is the measured quality variable, and y is the mean.

The closer the coefficient of determination (R^2) is to 1, the better the regression equation and the sample fit. Table 7 shows that the regression function fits well with the data for $R^2 = 0.94656$. Figure 9 shows the correlation between experimental data and the fitting data.

The goodness of fit test can only show the approximate degree of the model to the sample data. The linear relationship established between the explanatory variables and the explained variable in the model must be made a significant judgment in general by F-test, which is the variance analysis. The residual graphics is taken into account when analyzing the variance of the model, and it can be seen in Fig. 10. It is known from Fig. 10 that the distribution of the residues of the model follows a normal distribution approximately.

Table 8 shows results of variance analysis for the surface roughness R_a values of the narrow deep groove walls.

The quadratic polynomial regression model of surface roughness R_a value in the above was obtained at 95 % confidence level and the significant level α = 5 %. It is known from the Significance F column of Table 8 that the P value = 0.038574 < α. Therefore, the regression model is significant on the whole; thus, it can predict the roughness R_a values.

5 Conclusion

The creep feed grinding experiments designed by the orthogonal test method were carried out with a single-layer electroplated CBN wheel and SUS321 stainless steel workpiece. The narrow deep grooves were machined. The surface roughness/quality of each groove wall was analyzed. The influence of grinding parameters on the surface quality of the narrow deep grooves was explored, from which the prediction model of the surface roughness R_a value of the narrow deep groove walls of SUS321 stainless steel was established by partial least square regression.

The conclusions are summarized as follows:

(1) The feed rate has the greatest influence on the surface roughness R_a values of groove walls, the wheel speed has less influence on that, and the cutting depth has the smallest influence.
(2) The optimum combination is selected as $A_3B_1C_3$. The optimum parameters by orthogonal experiment optimum design are v_w = 1.5 mm/min, a_p = 5 mm, and n = 7000 rpm.
(3) It is desirable that the quadratic polynomial regression model of surface roughness R_a value was established by partial least square regression. The regression function fits well with the data for R^2 = 0.94656, and the model is significant on the whole with the data for P value = 0.038574 at 95 % confidence level.
(4) In order to prevent the grinding burn caused by the increase of grinding wheel speed, the problem of heat transfer in creep feed grinding should be considered in future grinding experiments.

Acknowledgments This work was financially supported by the National Natural Science Foundation of China (No. 51575375). And the authors are grateful to the anonymous reviewers for valuable suggestions and comments, which are very helpful for the improvement of this paper.

Table 8 Variance analysis for the surface roughness R_a values

	df	SS	MS	*F*	Significance *F*
Regression analysis	5	0.090708	0.018142	10.90142	0.038574
Residual	3	0.004992	0.001664		
Total	8	0.095701			

References

1. Wang YC, Tai BL, Loon MV, Shih AJ (2012) Grinding the sharp tip in thin NiTi and stainless steel wires. Int J Mach Tool Manu 62:53–60
2. Ohmori H, Katahira K, Komotori J, Mizutani M (2008) Functionalization of stainless steel surface through mirror-quality finish grinding. CIRP Ann Manuf Techn 57:545–549
3. Manimarana G, kumar MP, Venkatasamy R (2014) Influence of cryogenic cooling on surface grinding of stainless steel 316. Cryogenics 59:76–83
4. Zhou N, Peng RL, Pettersson R (2016) Surface integrity of 2304 duplex stainless steel after different grinding operations. J Mater Process Tech 229:294–304
5. Baptista R, Infante V, Branco CM (2008) Study of the fatigue behavior in welded joints of stainless steels treated by weld toe grinding and subjected to salt water corrosion. Int J Fatigue 30:453–462
6. Hadad M, Hadi M (2013) An investigation on surface grinding of hardened stainless steel S34700 and aluminum alloy AA6061 using minimum quantity of lubrication (MQL) technique. Int J Adv Manuf Technol 68:2145–2158. doi:10.1007/s00170-013-4830-3
7. Rudrapati R, Pal PK, Bandyopadhyay A (2016) Modeling and optimization of machining parameters in cylindrical grinding process. Int J Adv Manuf Technol 82:2167–2182. doi:10.1007/s00170-015-7500-9
8. Gopal AV, Rao PV (2003) Selection of optimum conditions for maximum material removal rate with surface finish and damage as constraints in SiC grinding. Int J Mach Tool Manu 43:1327–1336
9. Lin KY, Wang WH, Jiang RS, Xiong YF, Song GD (2016) Grindability and surface integrity of in situ TiB2 particle reinforced aluminum matrix composites. Int J Adv Manuf Technol. doi:10.1007/s00170-016-8841-8
10. Yao CF, Jin QC, Huang XC, Wu DX, Ren JX, Zhang DH (2013) Research on surface integrity of grinding Inconel718. Int J Adv Manuf Technol 65:1019–1030. doi:10.1007/s00170-012-4236-7
11. Fredj NB, Amamou R (2006) Ground surface roughness prediction based upon experimental design and neural network models. Int J Adv Manuf Technol 31:24–36. doi:10.1007/s00170-005-0169-8
12. Ohbuchi Y, Matsuo T, Sakat M (1995) Chipping in high-precision slot grinding of Mn-Zn ferrite. CIRP Ann Manuf Techn 44(1): 273–277
13. Webster J, Brinksmeier E, Heinzel C, Wittmann M, Thoens K (2002) Assessment of grinding fluid effectiveness in continuous-dress creep feed grinding. CIRP Ann Manuf Techn 1(1):235–240
14. Sunarto, Ichida Y (2001) Creep feed profile grinding of Ni-based superalloys with ultrafine-polycrystalline cBN abrasive grits. Precis Eng 25(4):274–283
15. Abdullah A, Pak A, Farahi M, Barzegari M (2007) Profile wear of resin-bonded nickel-coated diamond wheel and roughness in creep-feed grinding of cemented tungsten carbide. J Mater Process Tech 183:165–168
16. Aslan D, Budak E (2015) Surface roughness and thermo-mechanical force modeling for grinding operations with regular and circumferentially grooved wheels. J Mater Process Tech 223: 75–90
17. Wei LK, Huang XX, Huang ZZ, Zhou ZG (2013) Orthogonal test design for optimization of lipid accumulation and lipid property in Nannochloropsis oculata for biodiesel production. Bioresource Technol 147:534–538
18. Dong L, Sun YD, Li DJ (2010) Optimal deposition and layer modulation parameters for mechanical property enhancement of TiB2/Si3N4 multilayers using orthogonal experiment. Surf Coat Tech 205:s422–s425
19. Wu X, Leung DYC (2011) Optimization of biodiesel production from camelina oil using orthogonal experiment. Appl Energ 88: 3615–3624
20. Liang RJ (2008) Orthogonal test design for optimization of the extraction of polysaccharides from Phascolosoma esulenta and evaluation of its immunity activity. Carbohyd Polym 73:558–563
21. Malkin S (1989) Grinding technology—theory and applications of machining with abrasives, Society of Manufacturing Engineers, Dearborn, Michigan
22. Salmon SC (1992) Modern grinding process technology. McGraw Hill Inc., New York
23. Lopez F, Ibarra-Castanedo C, De Paulo Nicolau V, Maldague X (2014) Optimization of pulsed thermography inspection by partial least-squares regression. NDT&E Int 66:128–138